

A comparative study of multiscale geometric Analysis for SAR image compression

Amel Bouchemha

Department of Electrical Engineering, Faculty
of Engineering Sciences, University of
Tebessa, 12000, Algeria
bouchemha_amel@hotmail.fr

Mohamed cherif Nait-Hamoud

Department of Mathematics and Science
computing
University of Tebessa, 12000, ,Algeria
mc_naithamoud@hotmail.com

Noureddine Doghmane

Department of Electronics, Faculty of
Engineering Sciences, University Annaba,
23000, Algeria.
ndoghmane@univ-annaba.org

Abstract—The image representation in separable orthogonal bases cannot take advantage of geometrical regularity of image; which when explored efficiently improves the state of image compression. In this paper, we propose to experiment and compare an adaptive multiscale geometric decomposition for Synthetic Aperture Radar (SAR) image compression, called multiscale bandelets transform and an non adaptive multiscale geometric representation called Ridgelet transform. The second generation bandelets transform adopted in this work, is constructed in discrete domain with bandeletization of wavelet transform along the optimal direction of geometric flow that minimize the Lagrangian. We also discuss the criteria and results for evaluating the performances of SAR image compression using the wavelet, the bandelets and ridgelet transforms. Our experiments showed that during the compression phase, the speckle noise is removed from the SAR images inducing further improve of the coding efficiency .

Keywords- SAR image compression; bandelets transform; geometrical flow;

I. INTRODUCTION

Synthetic Aperture Radar (SAR) is active and coherent radar microwave, which produce high spatial resolution images from a moving platform. The ability of SAR sensors to acquire data in all weather conditions from very larger dynamic range, make them extremely attractive for diverse application such military or surveillance missions. With the improvement of SAR technology, the abundance of such imagery and due to the limited storage on the airplane or satellite, the data rate must be reduced without significant loss of image quality.

In the SAR image formation, the radar produces 2D (range and azimuth) terrain reflectivity images. The received radar signal is transform into In-phase (I) and Quadrature (Q) components to create the complex SAR image, via the Fourier transform and geometrical projections [1].

SAR images present special characteristics due to their acquisition mode. In addition to the speckle phenomenon resulting of coherent radiation, SAR images contain rich textures, revealing that there exist large homogeneous regions. So, for an efficient compression, we must use adaptive geometric transformations that can efficiently capture the

geometric regularity of sub-image.

The orthogonal wavelets allow efficient representation of homogeneous regularity in image like a homogeneous texture, or uniform regularity areas. However, they are not adapted to represent geometric regularity along the singularities of a surface because of their isotropic support. When explored this regularity yield an improvement of coding. The image representation in separable orthogonal bases cannot take advantage of geometrical regularity of image structure [2-6]. Several geometric representations have been proposed with good results in image analysis; like Bandelets transform [2-7], Contourlet transform, Ridgelet transform [8-10], Curvelet transform, which effectively capture the regular variation information in image along the local geometric direction. The Bandelet transform proposed by Erwan Le Pennec and Mallat [2,3], is an adaptive approximation of image geometry represented by a geometric flow, and it can represent the geometric regular images efficiently, this is due to the fact that the geometric flow indicates directions in which the image grey levels have regular variations. The Ridgelet Transform introduced by Candès and Donoho [8], is an non adaptive multiscale geometric decomposition, which permit to map a linear singularity in image into a point singularity using Radon transform, then the wavelet transform can be used to effectively handle the point singularity. For practical application such as image compression, it is necessary to have an orthonormal version of the Ridgelet transform for discrete and finite-size images. The Finite Ridgelet Transform (FRIT) is accomplished through the finite radon transform (FRAT)[10].

In this paper, we present a comparative study of the geometric multiscale transforms for SAR image compression. The paper is organized as follows: in the section 2, we describe a rapid implementation of geometric multiscale representation including the adaptive bandelets multiscale, the non adaptive finite ridgelet transforms and the algorithm of geometric based SAR image compression. The simulation results of progressive image compression on several SAR images are shown in section 3. Finally, the conclusion is drawn in section 4.

II. MULTISCALE SAR IMAGE COMPRESSION

A. Multiscale bandelets transform

The multiscale geometric decomposition provides an optimally basis for image representation that exploit the direction of geometric regularity, which mainly appear in the high frequency sub-bands of images. Bandelet bases are obtained with a *bandeletization* of warped wavelet bases, which takes advantage of the image regularity along the geometric flow $\vec{\tau}$ defined by a polynomial function. The bandelets transform can be considered as a wavelet basis deformed along the local direction (see Fig. 1(a)).

The bandelets transform divides the sub-bands of wavelet coefficient in dyadic squares inside which the geometric flow is parallel, using an optimization that eliminates the redundancy due to the wavelet transform. This segmentation is called decomposition quadtree (see Fig. 1(b)).

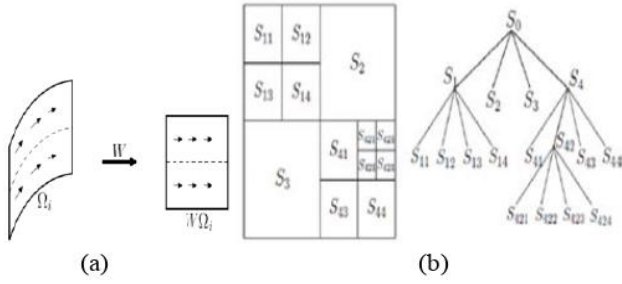


Fig. 1 (a) Example of deformation W of a region Ω_i , (b) Quadtree decomposition [2,3]

Firstly, the image f is divided into some region Ω_i . In a region Ω_i a geometric flow is a vector field $\vec{\tau}(x_1, x_2)$ that gives the regular variation direction of f in the neighborhood of each $(x_1, x_2) \in \Omega_i$ [2-8]. In each region, the first generation bandelets transform performs the following tasks:

1. Re-sampling that calculates the values of the image along the geometric flow. It is performed by interpolation on cubic splines,
2. Decomposition, if the region Ω_i is regular (without geometric flow) then the decomposition is carried out on a conventional biorthogonal wavelet basis using a bank of filters biorthogonal Daubechies 9/7. A separable discrete wavelet is defined by its mother wavelet ψ and its associated scaling function ϕ , written as :

$$\begin{cases} \phi_{j,m_1}(x_1)\psi_{j,m_2}(x_2) \\ \phi_{j,m_1}(x_1)\psi_{j,m_2}(x_2) \\ \psi_{j,m_1}(x_1)\psi_{j,m_2}(x_2) \end{cases} ; j \in \mathbb{Z}, (m_1, m_2) \in \mathbb{Z}^2 \quad (1)$$

Otherwise, if the region has a geometric flow $\vec{\tau}$, then the decomposition is performed on a wavelet basis deformed by a warping operator $W(\vec{\tau})$. The flow can be either parallel horizontally or vertically, the flow is then defined as:

$$\begin{aligned} \vec{\tau}_i(x_1, x_2) &= \vec{\tau}_i(x_2) = (c_i(x_2), 1) & \text{parallel horizontal flow} \\ \vec{\tau}_i(x_1, x_2) &= \vec{\tau}_i(x_1) = (1, c_i(x_1)) & \text{parallel vertical flow} \end{aligned} \quad (2)$$

The warped orthonormal basis for a parallel horizontal flow is defined by:

$$\begin{cases} \phi_{j,m_1}(x_1)\psi_{j,m_2}(x_2 - c(x_1)) \\ \phi_{j,m_1}(x_1)\psi_{j,m_2}(x_2 - c(x_1)) \\ \psi_{j,m_1}(x_1)\psi_{j,m_2}(x_2 - c(x_1)) \end{cases} ; (j, m_1, m_2) \in I_{W\Omega} \quad (3)$$

And hence, for a horizontal flow, the warped image is then:

$$Wf(x_1, x_2) = f(x_1, x_2 + c(x_1)) \quad (4)$$

3. Finally, the bandelization is performed, it exploit the regularity of the function along the geometric flow, by replacing the warped wavelet with orthonormal bandelets basis in the region Ω_i

A dyadic square segmentation is obtained by a successive subdivision of support image. The size of maximum and minimum dimension of image square affects the directions of geometric flow. Fig. 2 shows the geometric flows under different image partitions.

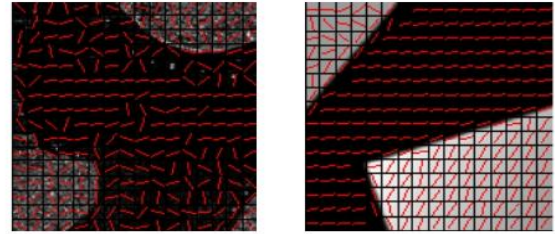


Fig. 2 Geometric flow under different dyadic square segmentation

B. Second generation bandelets

The first generation bandelets use advantageously the geometric structures of images. However, they are not directly defined in the discrete case, and they do not offer multi-resolution representation of the geometry. Therefore, Mallat et al. defined the second generation bandelets transform [2-5].

The second generation bandelets consists of applying a conventional orthogonal or biorthogonal wavelet transformation to image f , then, in each sub-band, a hierarchical dyadic square segmentation is performed under the best geometry representation. Thereafter, in each dyadic square, the best geometry which defines the directionality

should be determined. Next, an Orthogonal 1D projection is performed at the specified geometry to define a 1D discrete signal f_d . Finally, a 1D discrete wavelet transform is applied to the 1D signal f_d giving the bandelets coefficients b_k . The second generation bandelets representation of an image is illustrated in Fig. 3.

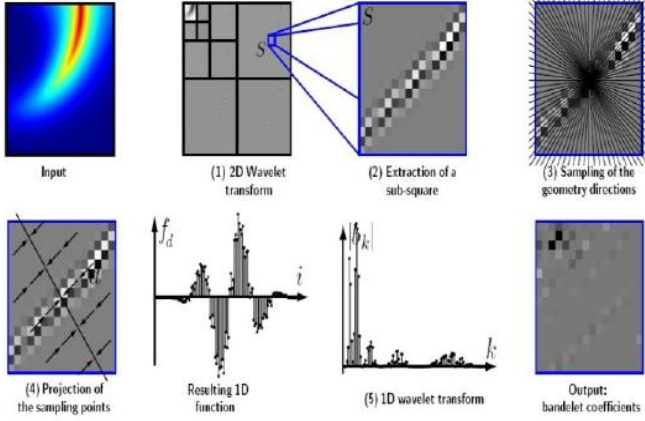


Fig. 3 Framework of the second generation of bandelets transform[2]

The best direction d , which produces the less approximation error between original image and the reconstructed image, is obtained by minimizing a cost function that is the Lagrangian value of the distortion rate, defined as:

$$\mathcal{L}(f, T) = \|f - f_R\|^2 + \lambda T^2 (R_G + R_B) \quad (5)$$

where f, f_R stand for the original image and the reconstructed image by bandelets coefficient; R_G, R_B represent respectively the number of bits to code geometric flow and bandelets coefficients in each square at scale 2^j ; $\lambda = 3/28$ is the Lagrangian factor and T is the threshold defined by user [2-6].

C. Finite Ridgelet Transform

Wavelets are known to be effective enough to represent objects with isolated point singularities but fail to represent line singularities. In order to overcome the weakness of wavelets in higher dimensions, Candes and Donoho have developed the continuous ridgelet transform. The Ridgelet transform is a wavelet analysis in the Radon domain. Indeed, linear discontinuities (lines) are projected as point singularities (points) by Radon transform. By applying wavelet transform on the various projections from Radon, we can get an optimal coding of the object outline within an image (see Fig. 4). Therefore, ridgelet transform is a representation of images using few coefficients, the most significant coefficient shows the directions of the image lines with the highest energy. Given an integrable bivariate function $f(x, y)$; its continuous Ridgelet transform (CRT) in \mathbb{R}^2 is defined as [8-10]:

$$CRT_f(a, b, \theta) = \int_{-\infty}^{+\infty} \int_{-\infty}^{+\infty} f(x, y) \psi_{a, b, \theta}(x, y) dx dy \quad (6)$$

Where $a = 2^j$ is the scale factor, b : the translation factor and $\psi_{a, b, \theta}(x)$: the ridgelets function in 2-dimensional which is defined from a wavelet mother function in 1-dimensional $\psi(x)$ as:

$$\psi_{a, b, \theta}(x) = a^{-1/2} \psi((x_1 \cos \theta + x_2 \sin \theta - b) / a) \quad (7)$$

In 2-D, points and lines are related via Radon transform. Thus the wavelet and ridgelet transforms are linked via the Radon transform. The Radon transform is the collection of line integrals, this is given as:

$$R_f(\theta, \tau) = \int_{\mathbb{R}^2} f(x) \delta(x_1 \cos \theta + x_2 \sin \theta - \tau) dx \quad (8)$$

The idea of the ridgelet transform of an object f is to map a line singularity into a point singularity using Radon transform, the 1-dimensional wavelet transform is applied to the slices of the Radon transform as:

$$CRT_f(a, b, \tau) = \int_{\mathbb{R}} \psi_{a, b}(\tau) R_f(\theta, \tau) d\tau \quad (9)$$

In image processing, it is necessary to have an orthonormal version of the Ridgelet transform for discrete and finite-size images. The finite ridgelet transform (FRIT) is accomplished through the finite radon transform (FRAT), which is defined as the summation of image pixel values along a set of lines. The discrete ridgelet transform FRIT is obtained by taking the discrete wavelet transform (DWT) of each FRAT projection $\text{set}(r_k(0), r_k(1), \dots, r_k(p-1))$, it is defined as:

$$FRIT(k, n) = \langle FRAT(k, m), \phi_n^k(m) \rangle \quad (10)$$

where $\phi_n^k(m)$ is the wavelet basis function of FRAT.

Consider $Z_p = \{0, 1, \dots, p-1\}$ the FRAT of real function $f(x, y)$ on the finite grid Z_p^2 is defined as:

$$r_k(m) = FRAT_f(k, m) = \frac{1}{\sqrt{p}} \sum_{(x, y) \in L_{k, m}} f(x, y) \quad (11)$$

where $L_{k, m}$ denotes a set of points that form a line on the lattice Z_p^2 , k : defines the slope of the line and m refers to the coefficient of ridgelet transform in each direction (see Fig. 4).

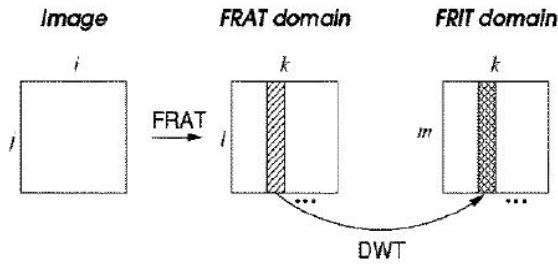


Fig. 4 The Finite Ridgelet Transform [8]

D. Image compression system based on transformation

Most compression systems can be decomposed into the components shown in Fig. 5. The transform is an essential lossless process which eliminates spatial redundancy which is a crucial step for compression. In most compression systems, the transform produces sets of coefficients that we refer to as coefficients sub-images. Given a desired total bit rate, the bit allocator determines how many bits should be allocated to each coefficient sub-image.

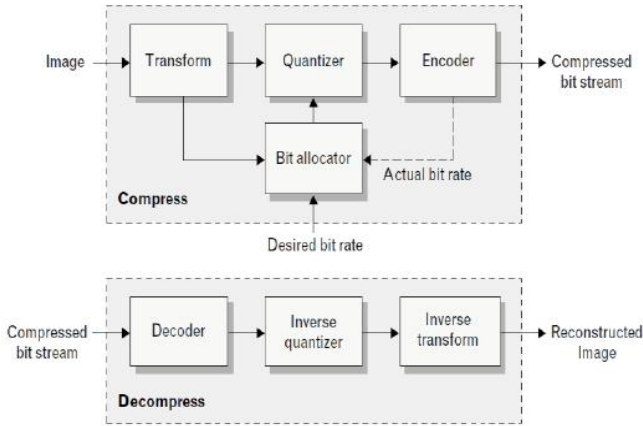


Fig. 5 Scheme of compression system based on the transform [1]

Analogically to the compression in wavelet basis, the bandelets transform and ridgelet transform codes are implemented with a scalar uniform quantization and entropy coding of all coefficients. Let $D = \{B^r\}_r$: the dictionary of all possible biorthogonal basis; for a fixed quantization step size, the best basis $\{b_m^r\}$ that minimizes the distortion-rate is found using Lagrangian optimization. The reconstructed image from the uniformly quantization with a threshold T_Q is given by:

$$f_R = \sum_{m=1}^{N^2} Q_{T_Q}(\langle f, b_m^r \rangle) b_m^r \quad (12)$$

The uniform quantize Q_{T_Q} , standing for the major source of loss in image quality converts the high-precision coefficients

into sets of discrete symbols by adaptive arithmetic coding procedures.

For a compressed image the bit rate achieved by the compressor measured in bit/pixel, is defined as the ratio of the number of bits used in the compressed representation of the image and the number of pixels in the image

E. Performance measures

The SAR images are corrupted by a noise called speckle, which makes the interpretation of SAR images very difficult. To evaluate SAR image compression techniques, the commonly used performance measures are : the peak signal to noise ratio (PSNR) defined as [11,12]:

$$PSNR(dB) = 10 \cdot \log \left(\frac{R^2 - 1}{MSE} \right) \quad (13)$$

Where MSE is the Mean Square Error $MSE = \sum_i \sum_k (f - f_R) / n \times m$ between the original image f of size (m,n) and the decompressed image f_R , R is the number of bits to code image ($R = 255$, for 8 bits/pixel)

The Equivalent Number of Looks (ENL) is used to measure the suppression of speckle noise in SAR image, it is calculated from the local variation coefficient C_v in a homogeneous zone. The ENL is defined as:

$$ENL = \frac{1}{C_v} = \frac{\mu^2}{\sigma^2} \quad (14)$$

Where μ and σ are respectively the mean and standard deviation estimated in the homogeneous zone

III. EXPERIMENT AND DISCUSS

In this section, we evaluate the performance of compression technique on several SAR images: Northrop Grumman SABR Radar SAR image of size 512x512, SAR image with mini-SAR (4meter in resolution) of sandia national laboratory of size 512x512 and Aerial image. To compare the compression results obtained using the second generation bandelets transform (2Gbadelet), the ridgelet transform and wavelet transform, we are required to use a visual estimation and quality measure for a fixed bit rate (bpp) to quantify the degree to which the reconstructed image matched the original.

The compression in a bandelet basis is compared with a compression in the 7/9 CDF (Cohen-Daubechies-Feauveau) wavelet basis and a compression in FRIT basis, using the same quantization and adaptive arithmetic coding procedures. Fig. 6, represents the compression results at several rate bit (bpp=0.28 bit/pixel and bpp=1.96 bit/pixel). In our work we use a uniform quantization with varying step. We note that there is a gain increase of about 1.32 dB at a bit rate of 1.96 bpp, and 4.57 dB at a bit rate 0.28 bpp over the wavelet transform.

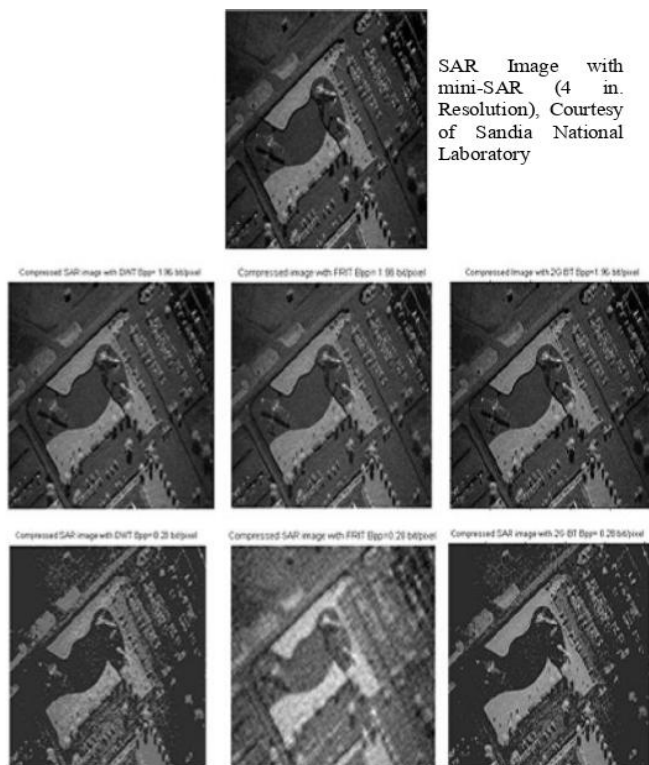


Fig. 6 Comparison of SAR image compression, at $\text{bpp}=1.96$ bit/pixel (DWT PSNR = 35.86 dB, FRIT PSNR = 34.71 dB and 2GBandelet PSNR = 37.18dB) and at $\text{bpp}=0.28$ bit/pixel (DWT PSNR = 19.55 dB, FRIT PSNR = 18.85 dB and 2G Bandelet PSNR = 24.10dB)

The artifact problem in 2G bandelet, wavelet and ridgelet transforms at the same rate is shown in fig. 7, the result demonstrate good visual quality with the least artifacts and fake structures in experiments using multiscale geometric transforms. The distortion is lower in a multiscale geometric basis than in a wavelet basis, which can be seen on the better reconstruction of the geometrical structures of the image.

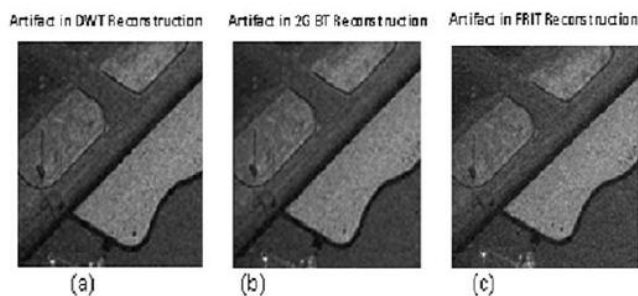


Fig. 7 Artifact problem in Wavelet, 2G Bandelet and FRIT transforms

The quantitative results are given in Table 1, which presents the values of the PSNR (dB) of compressed images at different rate bit.

TABLE 1. PSNR(dB) RESULTS FOR SAR IMAGE COMPRESSION AT DIFFERENT BPP (NUMBER BITS/PIXEL)

bpp (bit/pixel)	2.52	1.47	0.83	0.28	0.17	0.08
PSNR dB (DWT)	37.71	32.33	29.06	17.56	15.88	14.94
PSNR dB (2G BT)	38.86	33.18	30.01	17.19	15.39	14.07
PSNR dB (FRIT)	37.80	30.76	25.40	22.19	21.76	21.26

we notes that the PSNR -bit rates depend on the structural regularity of features present in each image. The Fig. 8 and 9 illustrate the variation of PSNR with bpp (bit/pixel) for several SAR images which have dominant geometric structures.

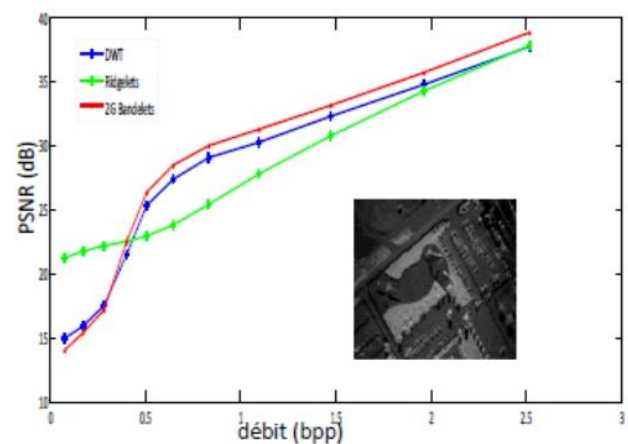


Fig. 8 Result of SAR image compression using 2G bandelet, Wavelet and FRIT transforms

For most images, the PSNR results obtained are in the range [25,40] dB for bit rate ranging between 0.1 and 2.55 bit per pixel. We notes that the PSNR rates obtained depend on the characteristics of the regularity of the structures present in each image.

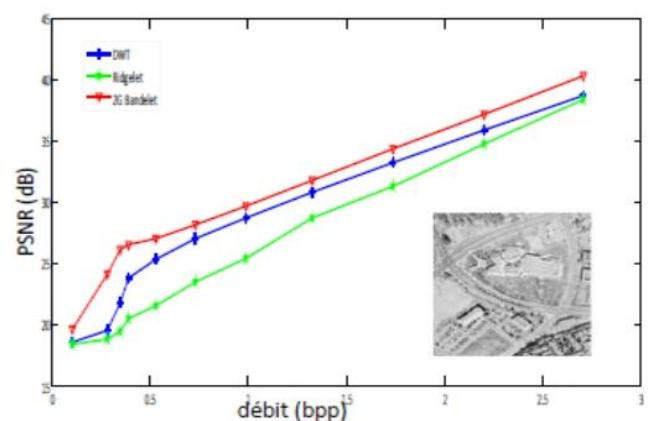


Fig. 9 Result of Aerial image compression using 2G bandelet, Wavelet and FRIT transforms

From the results shown in Fig. 10 below, we noted that in the case where the image has dominant directional structures; The geometric wavelets are robust and efficient; because they can better represent geometric regularities. While the separable wavelets are more suited to the representation of images where the homogenous areas are dominants (see Fig. 10).

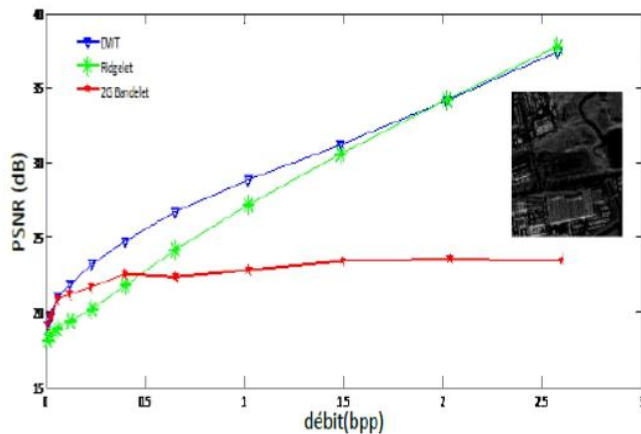


Fig. 10 Result of SABR Radar SAR image compression using 2G bandelet, Wavelet and FRIT transforms

One of the major problems in processing SAR image is speckle or coherent noise which can be modeled as multiplicative noise. A good filtering in homogeneous areas, is provided by a value of coefficient of variation C_v low, a decrease in the value of the standard deviation σ , an overall conservation of the mean μ , and an increase in the value of the ENL (see Table 2).

TABLE 2. EVALUATION MEASURE FOR SAR IMAGE COMPRESSION AND DESPECKLING

Bpp(bit/pixel) = 2.10			
	PSNR(dB)	ENL	C_v
2GBT	37.18	20.75	0.219
DWT	35.86	20.62	0.220
FRIT	34.71	20.75	0.219
Bpp (bit/pixel)=1.47			
2GBT	33.18	6.94	0.375
DWT	32.33	6.87	0.372
FRIT	30.76	6.93	0.379

IV. CONCLUSION

In this paper we present a comparative study of SAR images compression based on adaptive (2G Bandelets) and non adaptive (FRIT) geometric wavelet transforms with low complexity. We conducted our experiments on several SAR images. According to the objective evaluations criteria retained, namely PSNR and ENL, we note that a multiscale geometric representation for SAR image compression gives promising results of the rate of compression at low bit rate, and ensures an effective reduction of speckle noise. In the case

where the image has dominant directional structures; The geometric wavelets are robust and efficient ; because they can better represent geometric regularities. While the separable wavelets are more suited to the representation of images where the homogenous areas are dominants

REFERENCES

- [1] R. Baxter and M. Seibert, "Synthetic Aperture Radar Image Coding", lincoln laboratory journal vol.11, n° 2, 1998, pp. 121-158
- [2] E. Le Pennec and S. Mallat, "Sparse Geometric Image Representations with Bandelets", IEEE Trans. On image processing, vol. 14, n° 4, 2005, pp. 423-438.
- [3] E. Le Pennec and S. Mallat, "Bandelet image approximation and compression," SIAM J. Multiscale Modeling Simul. vol. 4, n° 3, pp. 992-1093, 2005.
- [4] S.Yang, Y.Lu, M.Wang and, L.Jiao , "Low bit rate SAR image coding based on adaptive multiscale Bandelets and cooperative decision", Signal Processing 89, 2009, pp. 1910-1920.
- [5] G. Peyre and S. Mallat, "Bandelets toolbox", available on Matlab Central, 2005.
- [6] X. Zhan, R. Zhang, D. Yin, and C. Huo,"SAR Image Compression Using Multiscale Dictionary Learning and Sparse Representation", IEEE GEO and remote sensing letters, vol. 10, n° 5, 2013, pp. 1090-1094.
- [7] Y. Shuyuan, P. DongLiang and W. Min, "SAR Image Compression based on Bandelet Network", Fourth International Conference on Natural Computation, 2008, pp. 559-563.
- [8] E.J. Candes, D.L. Donoho, " Ridgelets, a hey to higher dimensional intermittency", Phil. Transactions Royal Society of London A, pp 2495-2509, 1999.
- [9] Minh N. Do and Martin Vetterli, "Orthonormal Finite Ridgelet Transform for Image Compression", in proceedings of IEEE International Conference on Image Compressing, Vol. 2, pp. 367-370, September 2000.
- [10] M.N. Do and M. Martin, " The finite ridgelet transform for image representation", IEEE Trans.on image processing, Vol. 12, N°. 1, pp 16-28, 2003
- [11] X. Zhang and X. Jing, "Image denoising in contourlet domain based on a normal inverse Gaussian prior", Digital Signal Processing, vol. 20, pp. 1439-1446, 2010.
- [12] X. Yang, K. Wu and Y. Tang, "A new metric for measuring structure-preserving capability of despeckling of SAR images", ISPRS Journal of Photogrammetry and Remote Sensing, Vol.94, pp.143-15, 2014.